

# Interplay of Chemical Bonding and Magnetism in $\text{Fe}_4\text{N}$ , $\text{Fe}_3\text{N}$ and $\zeta - \text{Fe}_2\text{N}$

M. Sifkovits, H. Smolinski, S. Hellwig, and W. Weber  
*Institute of Physics, University of Dortmund, Germany*

Using spin density functional theory we have carried out a comparative study of chemical bonding and magnetism in  $\text{Fe}_4\text{N}$ ,  $\text{Fe}_3\text{N}$  and  $\zeta - \text{Fe}_2\text{N}$ . All of these compounds form close packed Fe lattices, while N occupies octahedral interstitial positions. High spin fcc Fe and hypothetical FeN with rock salt structure have been included in our study as reference systems. We find strong, covalent Fe–N bonds as a result of a substantial  $\sigma$ -type p–d hybridisation, with some charge transfer to N. Those Fe d orbitals which contribute to the p–d bonds, do no longer participate in the exchange splitting of the Fe d bands. Because of the large exchange fields, the majority spin d bands are always fully occupied, while the minority spin d bands are close to half-filling, thus optimizing the Fe d–d covalent bonding. As a consequence, in good approximation the individual Fe moments decrease in steps of  $\frac{1}{2} \mu_B$  from fcc iron ( $2.7 \mu_B$ ) via  $\text{Fe}_4\text{N}$  ( $2.7$  and  $1.97 \mu_B$ ),  $\text{Fe}_3\text{N}$  ( $1.99 \mu_B$ ) to  $\zeta - \text{Fe}_2\text{N}$  ( $1.43 \mu_B$ ).

## Keywords :

spin polarized density functional theory, chemical bonding, iron nitrides, itinerant magnetism

## PAC's :

75.50.-y; 75.50.Bb; 75.50.Ss

## Postal Address :

Prof. Dr. Werner Weber  
 Universität Dortmund, Institut für Physik  
 Lehrstuhl für theoretische Physik II  
 44221 Dortmund  
 FAX : ++49 0231 755 3569  
 Tel : ++49 0231 755 3563  
 E-mail : weber@fkt.physik.uni-dortmund.de

## I. INTRODUCTION

The nitrides of Fe have since long played an important role in steel technology. In particular, nitriding is used to harden iron surfaces and to passivate them against oxidation. On the other hand, the magnetic properties of some nitrides, especially those with small N contents, have raised considerable interest concerning magnetic data storage applications.

The phase diagram of  $\text{FeN}_x$  has been studied by the classic work of Jack [1,2]. Apart from the regions of very small N concentrations, such as  $\text{Fe}_{16}\text{N}_2$  (derived from the bcc iron), most ordered nitrides of Fe are based on close packed Fe structures.  $\text{Fe}_4\text{N}$  may be seen as fcc Fe, where  $\frac{1}{4}$  of all octahedral sites are occupied by N in such a way, that the octahedra share corners only. The structure of  $\text{Fe}_3\text{N}$  is based on a hexagonal close packed lattice of Fe, now with  $\frac{1}{3}$  of the octahedral sites being filled by N. Again, these are corner sharing octahedral units only. Finally, the  $\zeta - \text{Fe}_2\text{N}$  lattice is also based on hcp Fe, and  $\frac{1}{2}$  of the octahedral sites are occupied by N; now edge sharing arrangements appear as well.

In recent years, details of the  $\text{FeN}_x$  phase diagram, especially in the range between  $\text{FeN}_{0.3}$  and  $\text{FeN}_{0.5}$  have been investigated by Rechenbach et al. [3,4]. This study also includes neutron scattering data, which allow to extract the spatial distribution of the magnetic moment density.

Electronic structure calculations of the ordered iron nitrides based on spin density functional theory (SDFT) have been reported by various groups [5–9].

We employ the highly accurate full potential LAPW method of the WIEN95 program package [10]. For a systematic determination of ionic charges, we use the zero-flux charge density gradient method of Bader et al. [11]. In order to follow the trends in bonding and in magnetic properties through the series of nitrides, we include as references results for fcc Fe in the high spin state and also results for FeN in rock salt structure.

## II. CALCULATIONAL PROCEDURES

The structural parameters of the three nitrides were taken from experiment [3,4]. They are listed in table I. For our SDFT electronic structure calculations we used the local density approximation (LDA) and employed the exchange–correlation potential proposed by Perdew and Wang [12]. In all our calculations we used the same muffin–tin radii  $R_{\text{MT}}(\text{Fe}) = 1.7$  and  $R_{\text{MT}}(\text{N}) = 1.5$  atomic units. Typical energy cut–offs were between  $R_{\text{MT}}(\text{N}) * K_{\text{max}} = 8$  and 10. This corresponds to more than 150 plane waves per atom. For  $\text{Fe}_4\text{N}$  we used a k–mesh with 120 points in the irreducible part of the Brillouin zone, for  $\text{Fe}_3\text{N}$  and  $\zeta - \text{Fe}_2\text{N}$  the corresponding numbers have been 116 and 100 points. To accelerate self–consistency, we used a Fermi–factor smearing temperature  $T_{\text{FFS}} = 100$  K. For the determination of ionic charges by the zero–flux gradient method, a very fine real space mesh of the charge density  $\rho(\vec{r})$  was required. In fact each basis vector of the unit cell was divided into up to 400 intervals.

## III. RESULTS

### A. High spin fcc Fe

As a reference, we discuss the electronic structure of high spin fcc Fe (see Fig. 1) first. For the SDFT calculation, the lattice constant of  $\text{Fe}_4\text{N}$  was used. The majority spin d–bands are completely filled, while for the minority bands the Fermi energy lies close to the center of the d–bands in a local minimum of the density of states. Evaluating the exchange splitting of some typical d–band states we find  $\delta_{\text{E}_g}^{\text{AVG}} = 2.7$  eV. The magnetic moment is  $2.65 \mu_B$ . The s–band, which does not exhibit a large exchange splitting, is occupied by  $\approx 0.63$  electrons. The charge density (see Fig. 2) is rather spherical around the Fe atoms, yet there is some extra charge along the first nearest neighbour (1NN) Fe–Fe bond. This bonding charge is caused by the states of the half filled minority bands (where all bonding states are occupied). Note that the width of the minority d–bands is  $\approx 1$  eV larger than that of the (fully occupied) majority d–bands. This band widening, typical of all half–filled d–band materials (see, e.g. [13]), is another consequence of covalent d–d bonding in the minority bands. It is caused by the larger radial extent of the d wave functions at half band filling. In comparison, the majority d–band wave functions are somewhat contracted radially, as the anti–bonding states are filled as well. As a consequence the minority band wave functions extend further into the interstitial regions, resulting in the negative–spin densities there (see Fig. 3).

### B. $\text{Fe}_4\text{N}$

Only  $\frac{1}{4}$  of the octahedral sites are occupied by nitrogen atoms, and there are two inequivalent iron sites. If we put N on the  $(\frac{1}{2}, \frac{1}{2}, \frac{1}{2})$  position, there is one type of iron at (0,0,0) labeled Fe(I), and the other, Fe(II), at  $(\frac{1}{2}, \frac{1}{2}, 0)$ ,  $(\frac{1}{2}, 0, \frac{1}{2})$ , and  $(0, \frac{1}{2}, \frac{1}{2})$ .

In the density of states curves in Fig. 4 we can distinguish three band regions for both majority and minority spin bands. The lowest one is made up by the N 2p states which are rather strongly hybridized with the  $d(3z^2 - r^2)$  orbitals of the Fe(II) atoms through a  $(pd\sigma)$  type coupling. Then there follow d–bands, which show hardly any hybridisation with the N p orbitals. All of them are occupied in the majority spin bands. Above these d–bands there is the anti–bonding part of the p–d bands. Again, the Fermi level is situated close to the center of the d–band part of the minority spin.

The plot of the  $\text{Fe}_4\text{N}$  valence charge density(see Fig. 5) indicates the strong covalent Fe(II)–N bond. In comparison the bonding charge between Fe(I) and Fe(II) is by far less important. In a qualitative manner we may thus realize the extra stability provided by the addition of N as compared to the pure Fe lattice.

The spin density plot (Fig. 6) indicates that the dominant contributions to the spin density are located within the muffin–tin spheres. There are areas of negative moment density in the interstitial regions, which is again caused by the larger extension of the minority–spin wave functions. However, the total negative moment of those regions is rather small. The magnetic moments inside the muffin–tin spheres are listed in table III. They agree reasonably well with earlier work. We note a considerable decrease of the Fe(II) moment, as compared to fcc Fe, while the Fe(I) moment remains almost unchanged. There is a very small, negative moment at the N site.

The decrease of the Fe(II) moment may be explained in the following way : Because of the strong hybridisation of the  $d(3z^2 - r^2)$  orbitals with N  $p_z$  states, these  $d(3z^2 - r^2)$  states are occupied almost evenly in the majority and minority spin bands. Thus only 4 of the five d states are involved in the exchange splitting of  $\delta^{\text{AVG}} = 1.7$  eV. Full occupancy

in the majority spin bands and again half-filling in the minority spin bands (see Fig. 4) leads to a moment of  $\approx 2\mu_B$ . There is a considerable charge flow from Fe to N (see table II), as may have been expected from simple considerations concerning the center-of-mass positions of N(p) and Fe(3d) bands. Note that Fe(II) is more positively charged than Fe(I). From a tight-binding analysis of the SDFIT bands we find that the 4s partial density is reduced strongly on the Fe(II) site, and less so on the Fe(I) site. So we may attribute the charge flow (and the resulting positive charges on Fe(II) and Fe(I)) to the removal of s-type states on the Fe sites – more or less pronounced depending on the number of and distance to the N ligands.

### C. $\text{Fe}_3\text{N}$

In this hexagonal lattice, all Fe sites are equivalent, as are the N sites. Again the Fe atoms form octahedra around the N sites. These octahedra share corners in such a way that N sites of adjacent ab planes are connected via the corner Fe atoms. As a consequence, each Fe site has two nearest N neighbours. The Fe-N separation is very similar to  $\text{Fe}_4\text{N}$ , yet the N-Fe-N angle is now  $\approx 130^\circ$  instead of  $180^\circ$ . We note that the N sites in one specific ab plane are not connected via a N-Fe-N path.

The electronic DOS curves look quite similar to the  $\text{Fe}_4\text{N}$  case (see Fig. 7). The p-d band splitting and also the exchange splitting are very similar too, resulting in a magnetic moment on the Fe site of  $\approx 2\mu_B$ , practically the same value as for the Fe(II) site in  $\text{Fe}_4\text{N}$ . Again, this is in agreement with other studies. Each Fe site has two nearest N neighbours (separation very similar to  $\text{Fe}_4\text{N}$ ), now with an N-Fe-N angle of  $\approx 130^\circ$  instead of  $180^\circ$  in  $\text{Fe}_4\text{N}$ . We may construct on each Fe site a local d hybrid orbital with optimum  $\sigma$  coupling to both N neighbours. This d hybrid is admixed into the N(p) bands in a very similar way as is the  $d(3z^2 - r^2)$  orbital of Fe(II) into the N(p) bands of  $\text{Fe}_4\text{N}$ . It is not involved in the exchange split d-bands ( $\delta^{\text{AVG}} = 1.5 \text{ eV}$ ). Thus the remaining four d orbitals produce a moment of  $\approx 2\mu_B$ .

We also observe that the d minority spin bands are wider by  $\approx 0.8 \text{ eV}$  than the majority spin bands. This again results in negative moment densities in the interstitial regions. The N moment is negative and somewhat larger than in  $\text{Fe}_4\text{N}$ . We note that a similar negative value for N is also found in  $\zeta - \text{Fe}_2\text{N}$  (see table III). From Fig. 7 we realize that in the N(p) bands the ratio of p to d partial densities is larger for the minority bands (also observed for  $\zeta - \text{Fe}_2\text{N}$  and to a lesser extend for  $\text{Fe}_4\text{N}$ ). We attribute this effect to the larger energy difference between the centers of N(p) and Fe(d) bands in the minority spin case. This reduces p-d hybridisation there and enhances the p-type component over the majority spin case.

The charge density distribution is also very similar to  $\text{Fe}_4\text{N}$  – strong p-d bonding charge along the Fe-N bond and weaker Fe-Fe bonding. The resulting ionic charge of N has the same value as for  $\text{Fe}_4\text{N}$ , the Fe atoms are positively charged with values slightly larger than for the Fe(II) site of  $\text{Fe}_4\text{N}$ . Again, the charge flow can be attributed to the removal of s-type states on the Fe sites.

### D. $\zeta - \text{Fe}_2\text{N}$

This lattice type may be seen as a slightly distorted hexagonal structure. Again, there is only one type of Fe sites and one type of N sites. Like in  $\text{Fe}_3\text{N}$  the N centered octahedra share corners when the N atoms are situated in adjacent ab planes of the hexagonal lattice. Unlike  $\text{Fe}_3\text{N}$ , the N centered octahedra of one ab plane now share edges.

As a consequence, each Fe has 3 nearest N neighbours. If we try to construct a local basis with optimum  $\sigma$  coupling of Fe(d) hybrids to the N(p) orbitals, we require two hybrids. These are then excluded from the exchange split d-bands. Assuming again fully occupied majority and half-filled minority bands, we arrive at a moment of  $1.5 \mu_B$ . Looking at Fig. 10 we find this model reasonably well justified, although there are some deviations to the situation of  $\text{Fe}_3\text{N}$ : The exchange splitting is reduced down to  $\delta^{\text{AVG}} \approx 1.2 \text{ eV}$ , the anti-bonding p-d bands overlap slightly with the top of the pure d-bands and also the width of the minority spin bands ( $\approx 4.3 \text{ eV}$ ) is approaching the value of the majority spin bands ( $\approx 4.0 \text{ eV}$ ).

The charge density maps again indicate the bonding charge along the Fe(d) – N(p) bond. The N charge has decreased slightly in absolute value, indicating that the reservoir of s-type charge on the Fe atoms is almost exhausted.

## E. FeN, rock salt structure

Here, all adjacent N centered octahedra share edges. There are now six nearest neighbours of N to each Fe. The two d orbitals which exhibit  $\sigma$  coupling to N(p) are the  $E_g$  orbitals  $d(3z^2 - r^2)$  and  $d(x^2 - y^2)$ . Again, we may expect a moment of  $1.5 \mu_B$ , but we realize that the overlap of the anti-bonding  $E_g$  bands with the  $T_{2g}$  bands is quite significant. Also, the exchange splitting is further reduced down to  $\delta^{AVG} \approx 1.0 \text{ eV}$ , and, finally the excess width of the minority bands is smaller again. The negative charge at the N site is about the same as in  $\zeta - \text{Fe}_2\text{N}$ , but now all s-type charge density flow is exhausted, and a reduction of the d-type density is observed at Fe. Most of these effects help to reduce the Fe moment to  $\approx 1.1 \mu_B$ . Now the N moment is also positive. We attribute this effect to the above mentioned band overlap of the anti-bonding  $E_g$ -p bands and the  $T_{2g}$  bands. For the majority spin case, this leads to considerable extra majority spin density at N. There are still interstitial regions with negative moment density, these are now restricted to the tetrahedral interstitial sites, as all octahedral sites are occupied by N.

## IV. SUMMARY

There are clear trends seen in our study of  $\text{FeN}_x$  with close packed Fe lattices:

A) Bonding : N occupies octahedral sites. A strong covalent p-d bonding takes place in those octahedra, concomitant with charge transfer to N. These extra bonds clearly add stability to the Fe lattice. At low x values, the charge flow is predominantly fed by the s-type charge of the Fe sites, and the N excess charge is as high as -1.4. Values of that magnitude have been found in other compounds involving transition metals, such as  $\text{CaTaN}_2$  [14]. In nitrides with divalent simple metals or with noble metals [15], an even larger nitrogen charge of up to  $Z_N = -1.8$  has been found. With increasing N content, the N charge is more and more reduced down to a value of  $Z_N \approx -1.1$  for hypothetical FeN of rock salt structure.

B) Magnetism : There holds a rather simple rule through the series of Fe nitrides. The starting point is fcc Fe in the high spin state, carrying a moment of  $\approx 2.5 \mu_B$ . The five majority spin d-bands are completely filled (the case of a 'strong' ferromagnet), while the five minority states are half-filled, leading to a moment of  $5 \cdot \frac{1}{2} \mu_B$ .

In cubic  $\text{Fe}_4\text{N}$ , there are two inequivalent Fe sites. Fe(I) has the same nearest neighbour shell as in fcc iron, and keeps its moment. Fe(II) has two N nearest neighbours. Of the five d-orbitals, the  $d(3z^2 - r^2)$  shows strong  $\sigma$ -type coupling to N  $p_z$  (leading to the strong covalent bond discussed above). This orbital does not participate in the exchange splitting of the other d bands. Again, we find a 'strong' ferromagnet case, and the minority bands are half-filled. As a consequence, the magnetic moment of the Fe(II) site is reduced to  $4 \cdot \frac{1}{2} \mu_B$ .

In hcp  $\text{Fe}_3\text{N}$ , all the Fe sites are equivalent, with two nearest neighbours of N. Using a similar construction of the covalent bonds we again arrive at 4 exchange split bands per Fe and a moment of  $2 \mu_B$ .

In  $\zeta - \text{Fe}_2\text{N}$ , each of the equivalent Fe sites has three nearest neighbours of N. Now two d orbitals per Fe are involved in the covalent bonds, and the three remaining exchange split d bands per Fe yield a moment of  $\approx 1.5 \mu_B$ .

Even for hypothetical FeN with rock salt structure, this scheme holds approximately. Now there are six nearest nitrogen neighbours and the two  $E_g$  orbitals participate in the covalent bonds. Again a moment of  $\approx 1.5 \mu_B$  is expected from the  $T_{2g}$ -type Fe d bands. Yet the reduced exchange splitting and other effects reduce the moment to  $1.1 \mu_B$ .

Another notable effect is the large excess of the minority spin bandwidth over that of the majority spin bands, caused by the radially expanded d-orbitals of the half filled minority spin bands. One of the consequences is the appearance of negative-moment density in the octahedral and tetrahedral interstitial regions.

## ACKNOWLEDGMENTS

This work was supported by the DFG. Some of the calculations were performed on the Cray T3E of the Hochleistungsrechenzentrum Jlich and the IBM SP2 of the GMD.

---

[1] K.H. Jack "The iron-nitrogen system: The structures of  $\text{Fe}_4\text{N}$  and  $\text{Fe}_2\text{N}$ " Proc. Roy. Soc. **A 195**, 34 (1948)

- [2] K.H. Jack "The iron–nitrogen system: The crystal structures of epsilon–Phase iron nitrides " *Acta Cryst.* **5**, 404 (1952)
- [3] H.Jacobs, D. Rechenbach and U. Zachwieja "Structure determination of  $\gamma'$  –  $\text{Fe}_4\text{N}$  and  $\epsilon$  –  $\text{Fe}_3\text{N}$ " *Journal of Alloys and Compounds* **227**, 10 (1995)
- [4] D. Rechenbach and H. Jacobs "Structure determination of  $\epsilon$  –  $\text{Fe}_2\text{N}$  by neutron and synchrotron powder diffraction" *Journal of Alloys and Compounds* **235**, 15 (1996)
- [5] S. Matar, P. Mohn, G. Demazeau and B. Siberchicot "The calculated electronic and magnetic structure of  $\text{Fe}_4\text{N}$  and  $\text{Mn}_4\text{N}$ ", *J. Phys. France* **49**, 1761 (1988)
- [6] S. Matar, B. Siberchicot, M. Pénicaud and G. Demazeau "The electronic and magnetic properties of  $\text{Fe}_3\text{N}$ ", *J. Phys. I France* **2**, 1819 (1992)
- [7] S. Matar and P. Mohn "Electronic and Magnetic Properties of  $\text{Fe}_2\text{N}$  and  $\text{FeN}$  : Trends of the Magnetism of the Fe–N System ", *Active and Passive Elec. Comp.* **15**, 89 (1993)
- [8] A. Sakuma "Electronic and Magnetic Structure of  $\text{Fe}_4\text{N}$ " *J. Phys. Soc. Japan* **60**, 2007 (1991)
- [9] A. Sakuma "Self-consistent calculations for the electronic structure of Iron Nitrides  $\text{Fe}_3\text{N}$ ,  $\text{Fe}_4\text{N}$  and  $\text{Fe}_{16}\text{N}_2$ " *J. Magn. and Magn. Mat.* **102**, 127 (1991)
- [10] WIEN95, " Improved and updated Unix version of the original copyrighted WIEN–code, which was published by P. Blaha, K. Schwarz, P. Soratin and S.B. Trickey, in *Comput. Phys. Commun.* **59** 399 (1990)"
- [11] R.F.W. Bader and P.M. Beddall, "Virial Field Relationship for Molecular Charge Distributions and the Spatial Partitioning of Molecular Properties", *J. Chem. Phys.* **56**, 3320 (1972)
- [12] J. P. Perdew and Y Wang, "Accurate and simple analytic representation of the electron–gas correlation energy ", *Phys. Rev. B* **45**, 13244 (1992)
- [13] V.L. Moruzzi, J.F. Janak and A.R. Williams "Calculated Electronic Properties of Metals ", Pergamon Press 1978
- [14] H. Smolinski and W. Weber, to be published in *Z. Phys. B*, special issue for the 11<sup>th</sup> Workshop of the ISSSP.
- [15] U. Hahn and W. Weber "Electronic structure and chemical–bonding mechanism of  $\text{Cu}_3\text{N}$ ,  $\text{Cu}_3\text{NPd}$  and related Cu(I) Compounds", *Phys. Rev. B* **53**, 12684 (1996)
- [16] Chen et al., *J. Phys. Chem.* **87**, 5326 (1983)
- [17] B.J. Kooi et al., *Materials Transactions* **25A** 2797 (1994)
- [18] K. Suzuki, H. Morita, T. Kneko, H. Yoshida and H. Fujimori, *Journal of Alloys and Compounds* **201** 11 (1993)
- [19] M. Takahashi and Y. Kawazoe, *The Science reports of the Research Institutes Tohoku A* **41** 141 (1996)

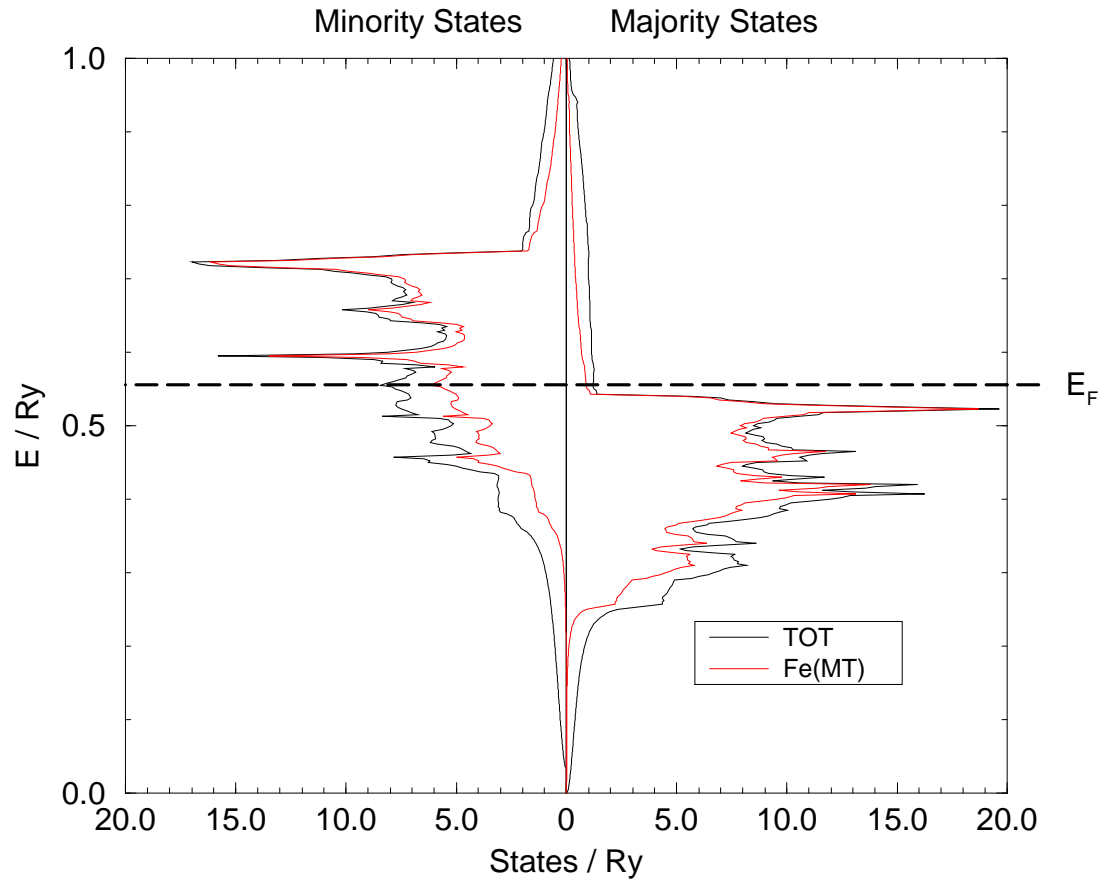


FIG. 1. Total density of states for high spin fcc Fe.

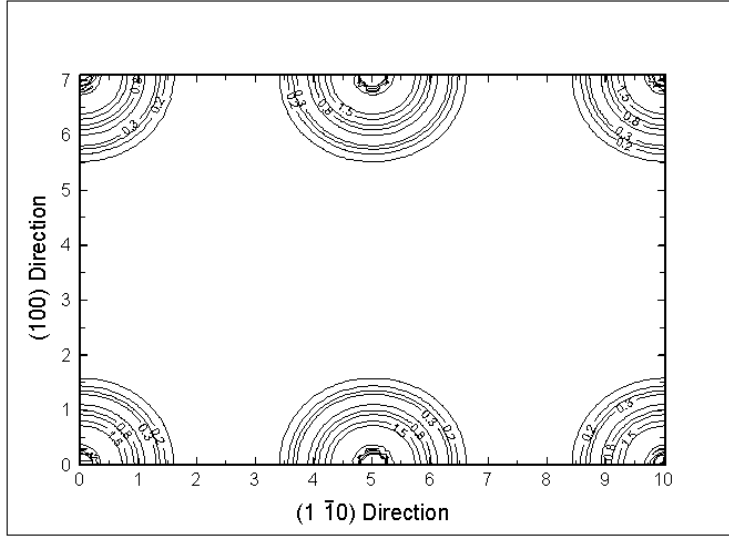


FIG. 2. Valence charge density of fcc Fe in the  $(1\bar{1}0)$  plane in units of  $e/(\text{atomic units})^3$ . The length scales are also in a.u.

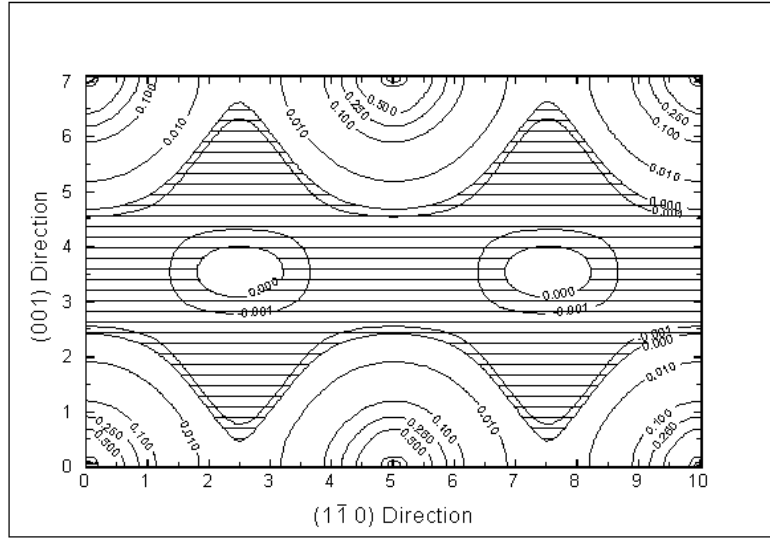


FIG. 3. Spin density of fcc Fe in the  $(1\bar{1}0)$  plane in units of  $e/(\text{a.u.})^3$ . Areas of negative-spin density are hatched.

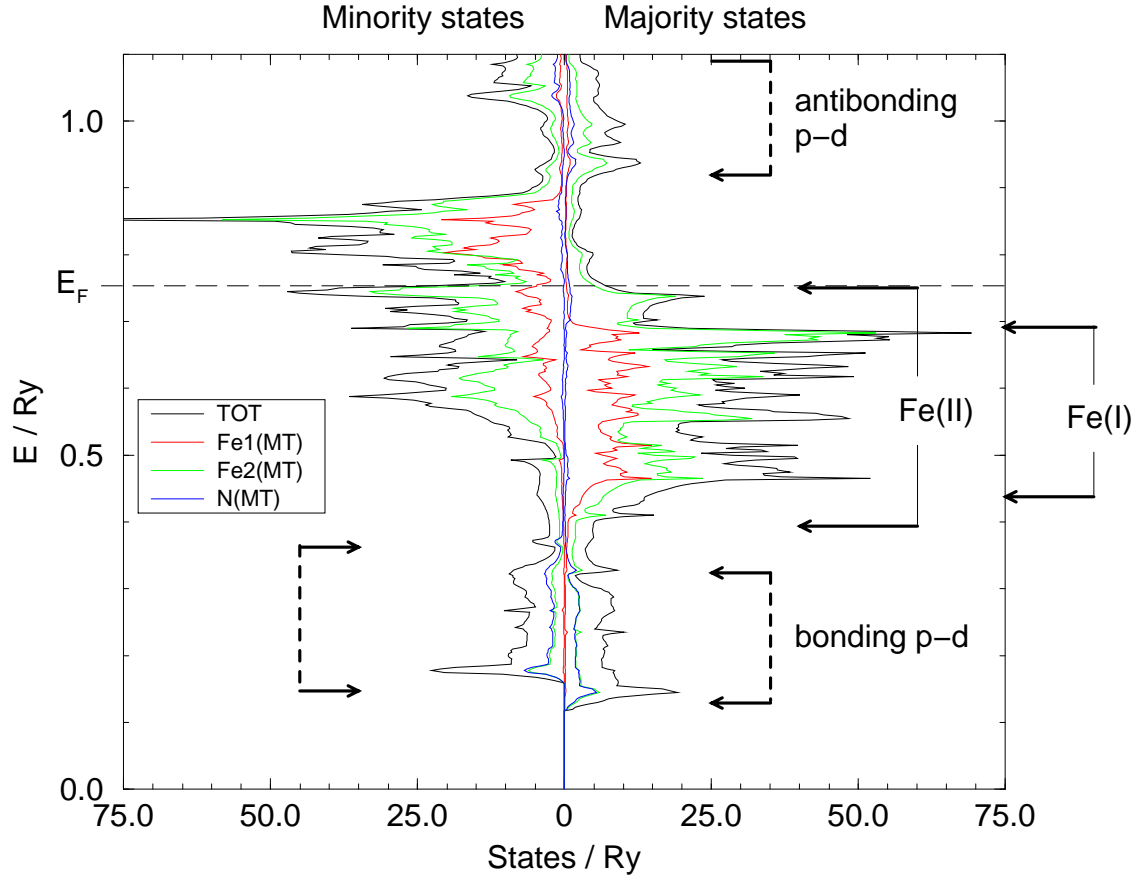


FIG. 4. Total (TOT) and muffin-tin projected (MT) densities of states for  $\text{Fe}_4\text{N}$ . Colours indicate MT orbital partial densities.



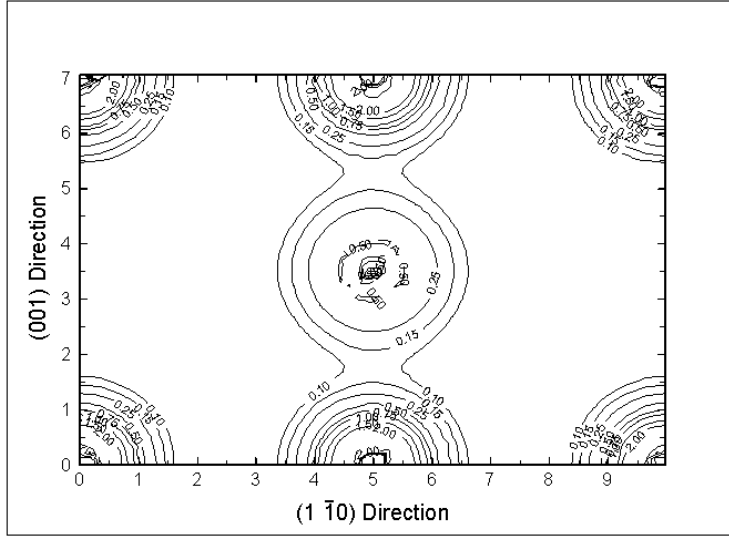


FIG. 5. Valence charge density of  $\text{Fe}_4\text{N}$  in the  $(1\bar{1}0)$  plane.

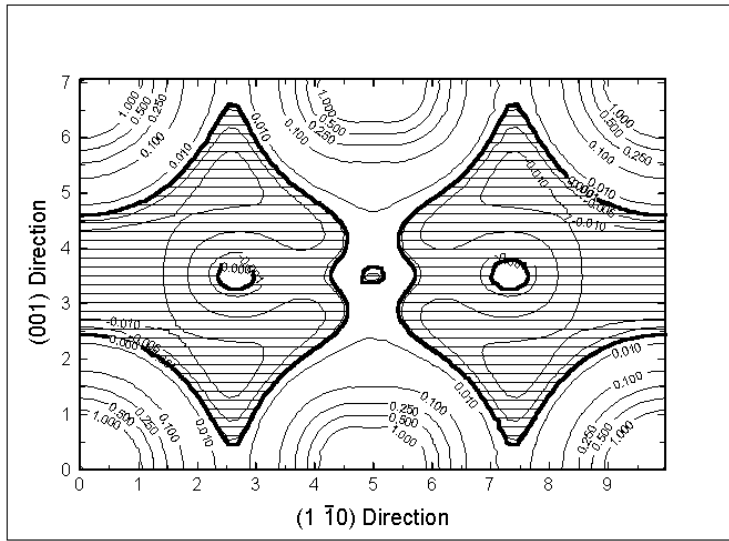


FIG. 6. Spin density of  $\text{Fe}_4\text{N}$  in the  $(1\bar{1}0)$  plane.

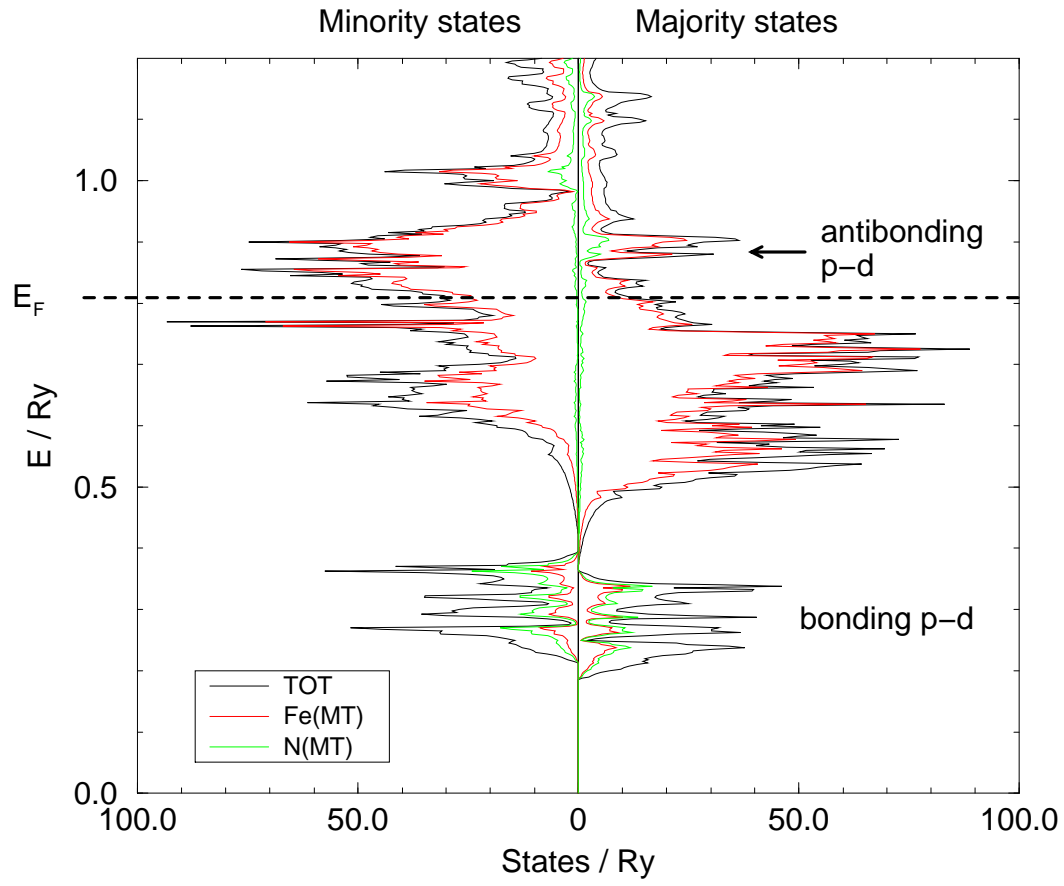


FIG. 7. Total and muffin-tin projected densities of states for  $\text{Fe}_3\text{N}$ .

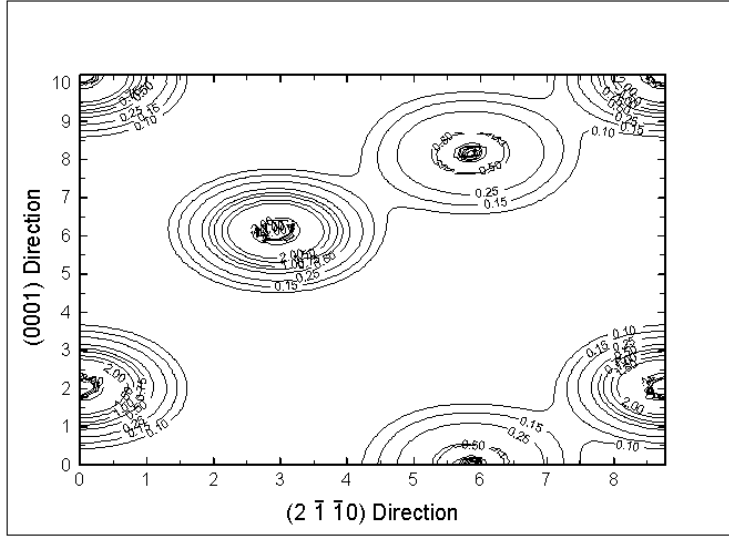


FIG. 8. Valence charge density of Fe<sub>3</sub>N in the (0330) plane. The N atoms are lying in the plane, while the Fe atoms are centered slightly above.

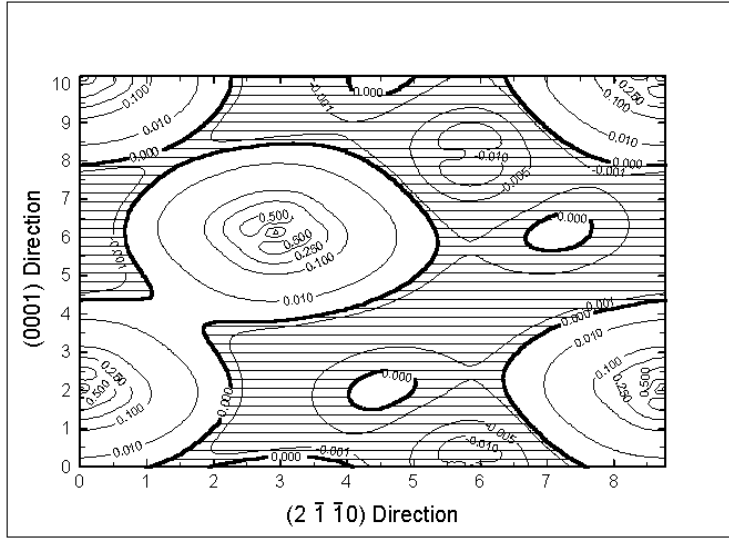


FIG. 9. Spin density of Fe<sub>3</sub>N in the (0330) plane.

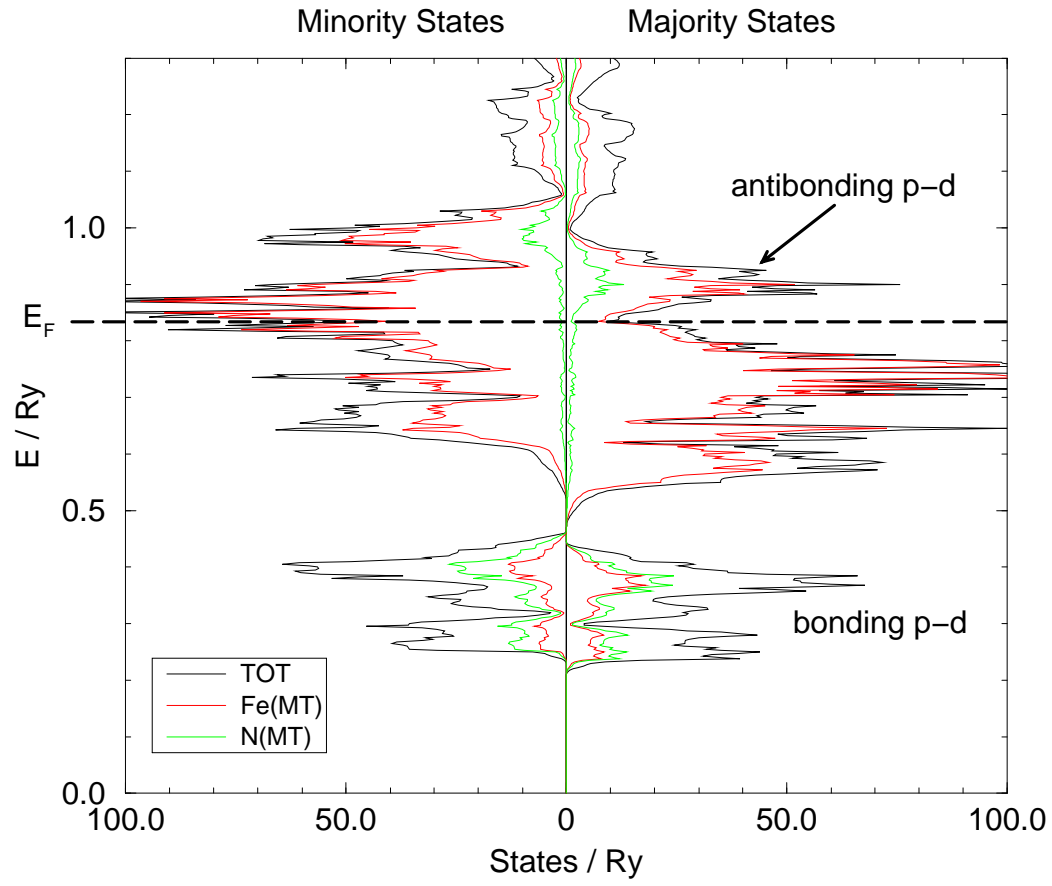
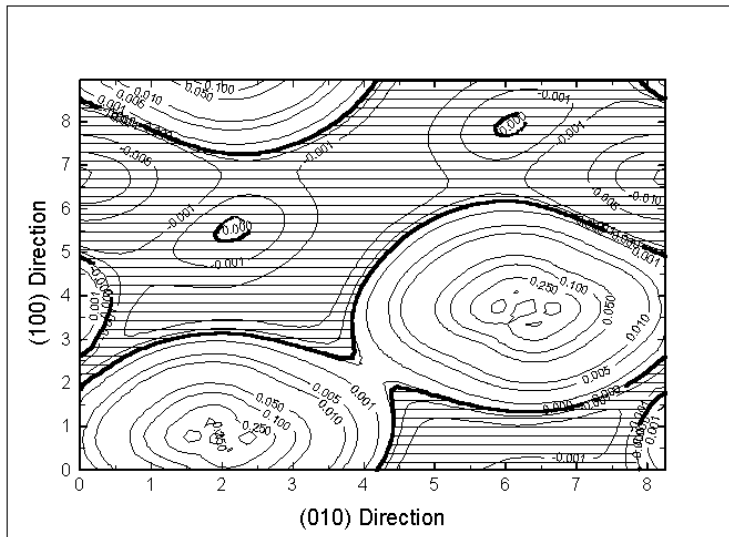
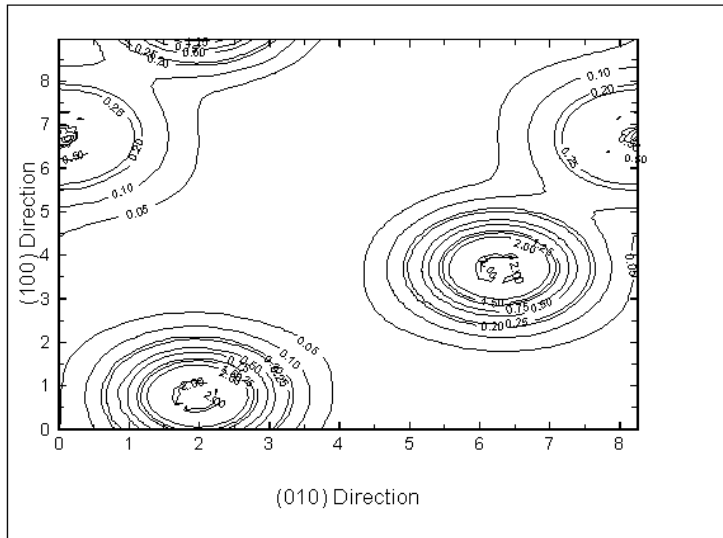


FIG. 10. Total and muffin-tin projected densities of states for Fe<sub>2</sub>N.



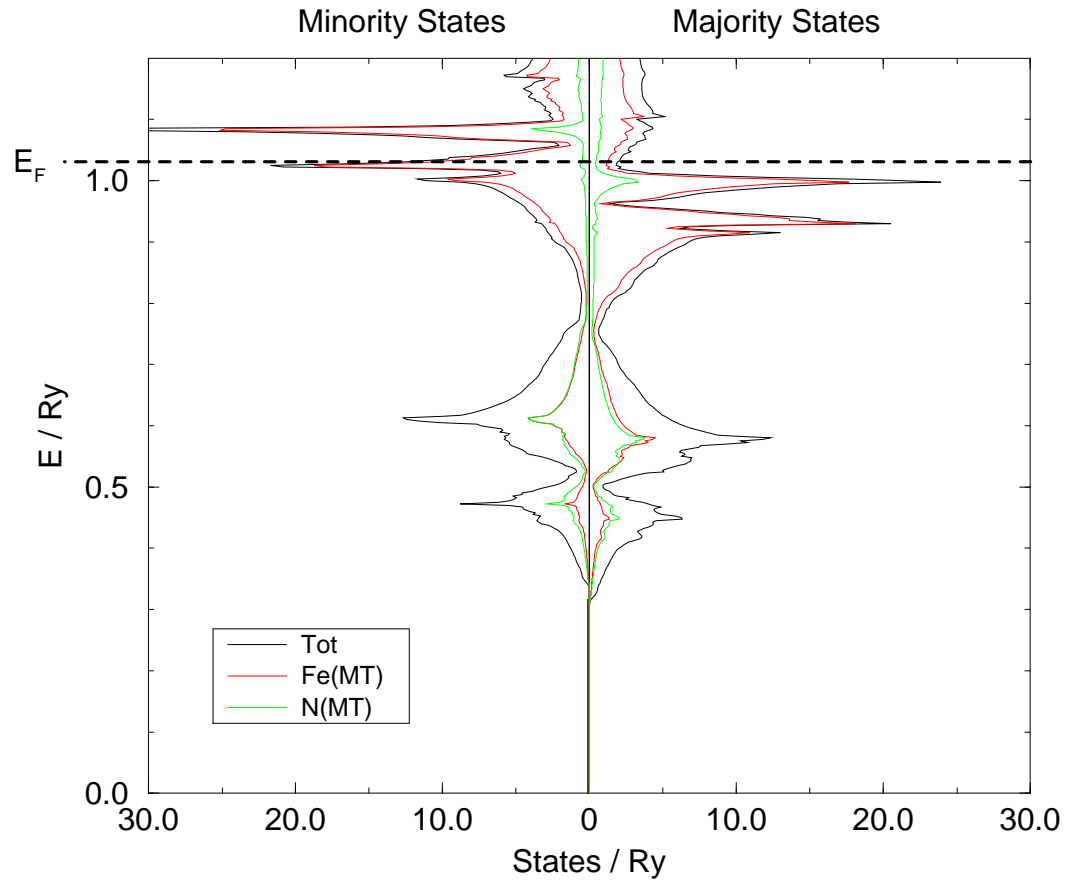


FIG. 13. Total and muffin-tin partial densities of states for FeN in the rocksalt structure.

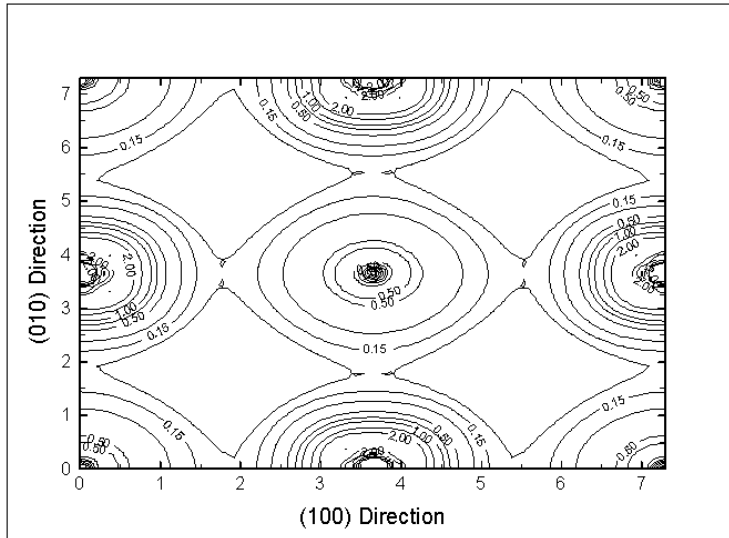


FIG. 14. Valence charge density of FeN(NaCl) in the (100) plane.

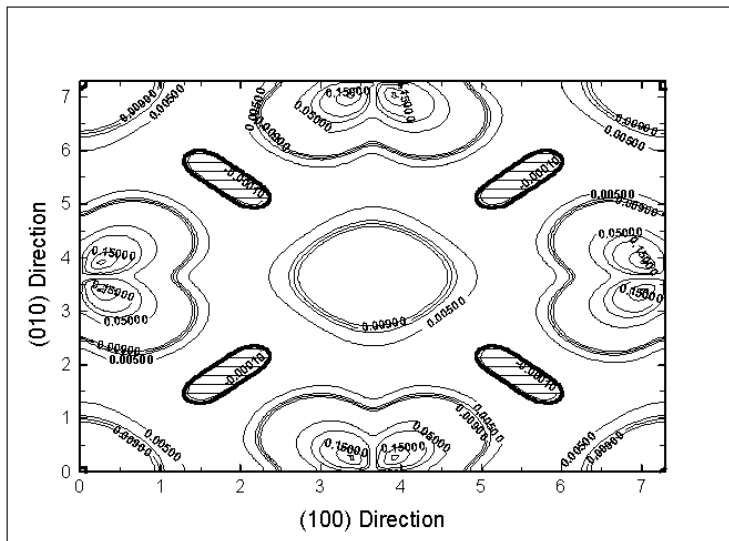


FIG. 15. Spin density of FeN(NaCl) in the (100) plane.

TABLE I. Structures and lattice parameters of the various iron nitrides. All lengths are given in atomic units (a.u.).

Material	space group	a / a.u.	b / a.u.	c / a.u.	Fe(I)	Fe(II)	N
Fe <sub>4</sub> N	Pm3m	7.1707	7.1707	7.1707	3d ( $\frac{1}{2}, 0, 0$ )	1b ( $\frac{1}{2}, \frac{1}{2}, \frac{1}{2}$ )	1a (0,0,0)
Fe <sub>3</sub> N	P6 <sub>3</sub> 22	8.8694	8.8694	8.2552	–	6g (0,0.325,0)	2c ( $\frac{1}{3}, \frac{2}{3}, \frac{1}{4}$ )
$\zeta$ – Fe <sub>2</sub> N	Pbcn	8.3881	10.4751	9.1548	–	8d (0.251,0.128,0.008)	4c (0,0.864,0.25)
FeN	Fm3m	7.372	7.372	7.372	–	4a (0,0,0)	4b ( $\frac{1}{2}, \frac{1}{2}, \frac{1}{2}$ )

TABLE II. Ionic charges as determined by the method of Bader. Also shown are charges of previous work, derived from the (overlapping) muffin–tin occupation numbers.

Material	Charges		
	Fe(I)	Fe(II)	N
Fe <sub>4</sub> N	+0.2	+0.4	-1.4
Fe <sub>4</sub> N <sup>a</sup>	+1.04	+0.51	+0.02
Fe <sub>3</sub> N	–	+0.47	-1.4
Fe <sub>3</sub> N <sup>b</sup>	–	-0.02	+0.95
$\zeta$ – Fe <sub>2</sub> N	–	+0.6	-1.2
$\zeta$ – Fe <sub>2</sub> N <sup>c</sup>	–	-0.23	+0.89
FeN	–	+1.1	-1.1

<sup>a</sup>Ref. [5]

<sup>b</sup>Ref. [6]

<sup>c</sup>Ref. [7]

 TABLE III. Muffin–tin magnetic moments of the various materials. We also give the results of previous work. All magnetic moments are given in units of  $\mu_B$ .

Material	Muffin–tin moment		
	Fe(I)	Fe(II)	N
Fe <sub>4</sub> N	2.73	1.97	-0.005
Fe <sub>4</sub> N <sup>a</sup>	2.98	1.79	0.02
Fe <sub>3</sub> N	–	1.99	-0.06
Fe <sub>3</sub> N <sup>b</sup>	–	1.96	-0.05
$\zeta$ – Fe <sub>2</sub> N	–	1.43	-0.06
$\zeta$ – Fe <sub>2</sub> N <sup>c</sup>	–	1.49	-0.07
FeN	–	1.15	0.08

<sup>a</sup>Ref. [5]

<sup>b</sup>Ref. [6]

<sup>c</sup>Ref. [7]